Carbohydrate Research 344 (2009) 355–361

Contents lists available at ScienceDirect

Carbohydrate Research

journal homepage: www.elsevier.com/locate/carres

Examination of the effect of structural variation on the N-glycosidic torsion (Φ_N) among *N*-(β-D-glycopyranosyl)acetamido and propionamido derivatives of monosaccharides based on crystallography and quantum chemical calculations

Mohamed Mohamed Naseer Ali [a,†,‡], Udayanath Aich [b,§,†], Serge Pérez [a], Anne Imberty [a,*], Duraikkannu Loganathan [b,*]

[a] CERMAV-CNRS,[¶] Domaine Universitaire de Grenoble, BP 53, F-38041 Grenoble, France
[b] Department of Chemistry, Indian Institute of Technology Madras, Chennai 600036, India

ARTICLE INFO

Article history:
Received 26 September 2008
Received in revised form 6 November 2008
Accepted 6 November 2008
Available online 6 December 2008

Keywords:
N-Glycoprotein
Crystallography
Quantum chemistry

ABSTRACT

GlcNAcβAsn linkage is conserved in the N-glycoproteins of all eukaryotes. L-Glutamine (Gln), which is a one carbon higher homolog of Asn, is never glycosylated. X-ray crystallographic study of several β-1-*N*-acetamido- and propionamido derivatives of monosaccharides has earlier shown that the N-glycosidic torsion, Φ_N, is influenced to a larger extent by the structural variation of the sugar part than that of the aglycon moiety. In order to examine the influence of the carbohydrate pendent groups on the conformational preference of the N-glycosidic linkage with respect to Φ_N, several models and analogs with *gluco* and *manno* configuration have been studied in the present work by computational chemistry. The crystal structure of XylβNHPr is reported here and its molecular packing compared with related analogs. The conjunction of combining Crystallographic and computational studies allows to demonstrate the strong influence that the group at C2, and environmental factors particularly inter- and intramolecular interactions involving regular hydrogen bonds and the weak C–H···O contacts, have on the energy preference of the Φ_N torsion angle.

1. Introduction

Glycan components of glycoproteins play key roles in many biological processes.[1,2] The linkage region constituents, 2-acetamino-2-deoxy-β-D-glucopyranose monosaccharide (GlcNAc) and L-asparagine amino acid (Asn), are conserved in N-glycoproteins of all eukaryotes, whereas L-glutamine amino acid (Gln) that possesses a very similar side chain is never glycosylated.[3] Elucidation of the structure and conformation of the linkage region of glycoproteins are of fundamental importance to understand the presentation and dynamics of the carbohydrate chain at the protein surface. While crystallography and NMR studies of glycoproteins provide statistical data of interest,[4,5] the analysis of models and analogs is required for the precise structural characterization. For this purpose, a major program has been focused on the synthesis, the crystallography, and more recently the ab initio calculations of several *N*-β-glycosyl amides.[6–11] Among the models and analogs examined earlier,[6] the acetamido derivatives of Man and Xyl showed Φ_N (O5–C1–N1–C1′) values of −114.5° and −121.2°, respectively, with maximum deviation from the value of −89.8° reported for the model compound GlcNAcβNHAc (Chart 1), revealing the effect of the sugar structure on Φ_N. On the other hand, the Φ_N values, −91.0° and −89.5°, of the propionamido derivatives of GlcNAc and Glc (analogs of the unnatural GlcNAcβGln and GlcβGln, respectively) matched well with those (−93.8° and −89.8°) reported for their corresponding acetamido derivatives.[10,11] These data suggest that Φ_N is influenced to a larger extent by the structural variation of the sugar part rather than that of the aglycon moiety.

As a logical extension of the above systematic investigation, the present work was undertaken to prepare and examine the crystal structures of the propionamido derivatives of Man and Xyl. Comparative analysis of crystal structures of haloacetamido derivatives[9] with those reported for GlcNAcAsn[12,13] highlighted the influence of the sugar ring substituents and the aglycone moiety

* Corresponding authors. Tel.: +33 04 76 03 7636; fax: +33 4 7654 7203 (A.I.).
E-mail addresses: Imberty@cermav.cnrs.fr (A. Imberty), loganath@iitm.ac.in (D. Loganathan).
† These two authors participated equally to the work.
‡ Present address: Department of Geosciences, The Pennsylvania State University, University Park, PA 16802, USA.
§ Present address: Department of Biomedical Engineering, Johns Hopkins University, Baltimore, MD 21218, USA.
¶ Affiliated to Université Joseph Fourier and belonging to ICMG.

0008-6215/$ - see front matter © 2008 Elsevier Ltd. All rights reserved.
doi:10.1016/j.carres.2008.11.013

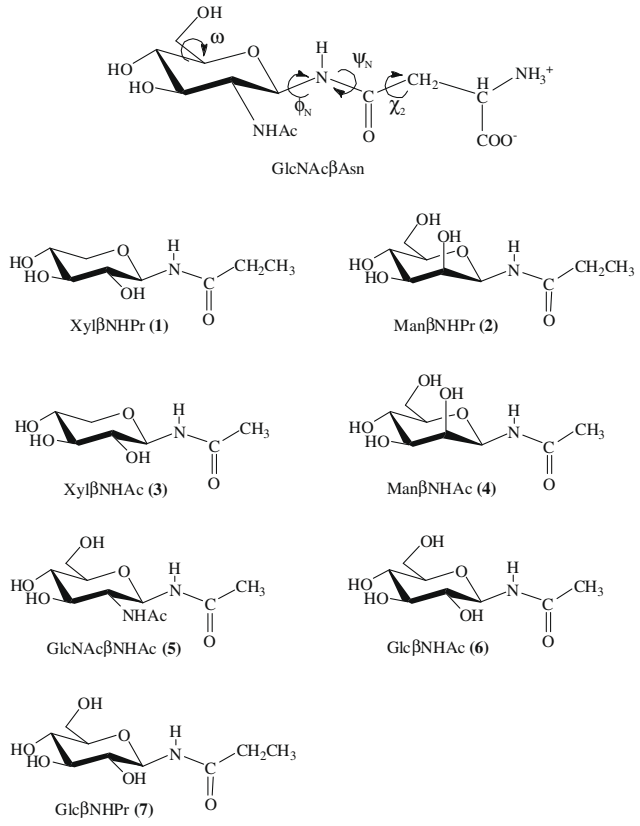

Chart 1. Structures of compounds **1**–**7** and of GlcNAcβAsn.

on χ_2 (N1–C1′–C2′–X) torsion angle at the *N*-glycosidic linkage. Our recent DFT and ab initio calculations on the preferred conformation as defined by the χ_2 torsion angle, combined with the above comparative crystallographic analysis, provided arguments for the structural effect of the *N*-acetyl group at C2 in establishing an extended conformation that orients the oligosaccharide away from the protein surface.[9] In order to analyze the effect of the aglycon substituent on the conformational preference of the Φ_N torsion angle, ab initio calculations have been performed in the present study on compound **1** and its N-acetylated analog (**3**). The influence of ring substituents at C2 and at C5 have also been analyzed by performing these calculations on compounds **3**–**7** (Chart 1) that display *gluco* and *manno* configurations of the ring.

2. Experimental

2.1. General

Thin layer chromatograms were performed on 25 mm E. Merck silica gel plates (60F-254). Detection was done by spraying the plates with 10% sulfuric acid in ethanol and heating on a hot plate. Optical rotation was measured at 30 °C on a JASCO-DIP 200 digital polarimeter using a cell of 10 mm length. NMR spectra were recorded on a Bruker AV400 spectrometer. ESIMS spectra were measured on a Micromass Q-Tof mass spectrometer.

2.2. General procedure for the preparation of *N*-(β-D-glycopyranosyl)propionamides

To a solution of β-D-glycopyranosylamine[14] (30 mmol) in dry methanol (25 mL) cooled to 0 °C, propionic anhydride (6.51 g, 50 mmol) was added, in portions, and the reaction mixture stirred for 2 h at 0 °C, followed by stirring at room temperature overnight. The solid separated out from the solution, which was filtered, washed with cold methanol, and recrystallized from aqueous methanol (3:2) to give crystalline solid.

2.2.1. *N*-(β-D-Xylopyranosyl)propionamide (1)

From β-D-xylopyranosylamine (4.47 g); crystals (aqueous methanol), 3.81 g (62%); mp 209 °C, $[\alpha]_D$ = +14.2 (*c* 1, water); IR (KBr) 3228, 2960, 2928, 1651, 1545, 1456, 1392, 1254, 1136, 1065, 1040, 985, 787 cm^{-1}; ^1H NMR (400 MHz, D_2O) δ 4.84 (d, 1H, *J* = 8.8 Hz, H-1), 3.89 (dd, 1H, *J* = 11.2, 5.4 Hz, H-5), 3.58 (m, 1H, H-4), 3.45 (t, 1H, *J* = 9.0 Hz, H-3), 3.40–3.30 (m, 2H, H-2 and H-5b), 2.29 (q, 2H, $-CH_2$), 1.07 ppm (t, 3H, $-CH_3$) ppm; ^{13}C NMR (100 MHz, D_2O) δ 179.4 (–CO–), 79.9 (C-1), 76.5, 71.6, 69.0, 66.7, 29.0 (CH_2), 9.1 ppm ($-CH_3$); HRESIMS: Calcd for $C_8H_{15}NO_5Na$ $[M+Na]^+$: 228.0848. Found: *m*/*z*: 228.0855.

2.2.2. *N*-(β-D-Mannopyranosyl)propionamide (2)

From β-D-mannopyranosylamine (5.37 g); 4.16 g (59%), mp 198 °C, $[\alpha]_D$ = −41.2 (*c* 1, water); IR (KBr) 3366, 2983, 2942, 1648, 1528, 1457, 1376, 1311, 1228, 1142, 1074, 1059, 789 cm^{-1}; ^1H NMR (400 MHz, D_2O) δ 5.13 (s, 1H, H-1), 3.86 (m, 1H, H-2), 3.82 (dd, 1H, *J* = 2.0, 12.0 Hz, H-6a), 3.68–3.60 (m, 2H, H6-b and H-3), 3.52 (t, 1H, *J* = 9.8 Hz, H-4), 3.39 ppm (m, 1H, H-5), 2.30 and 2.24 (m each, 2H, $-CH_2$), 1.04 ppm (m, 3H, $-CH_3$) ppm; ^{13}C NMR (100 MHz, D_2O) δ 176.5, 77.8 (C-1), 77.7, 73.5, 70.3, 66.5, 61.0 (C-6), 29.0 ($-CH_2$), 9.2 ppm ($-CH_3$); HRESIMS: Calcd for $C_9H_{17}NO_6Na$ $[M+Na]^+$: 258.0954. Found: *m*/*z*: 258.0960.

2.3. Preparation of single crystals and X-ray crystallographic analysis

Compound **1** was crystallized from aqueous methanol at room temperature. X-ray diffraction data were collected at room temperature in the ω–2θ scan mode on an Enraf-Nonius CAD4 diffractometer equipped with a Mo source. The relevant details of data collection and refinement are given in Table 1. The structure was solved by direct methods using SHELXS-97, and the refinement was done by full matrix using SHELXL-97.[15] ORTEP and packing diagrams were drawn using PLATON[16] and Mercury 1.4.2. (CCDC, Cambridge).

Table 1
Data collection and refinement statistics for XylβNHPr (**1**)

Parameter	Compound **1**
Empirical formula	$C_8H_{15}NO_5$
Formula weight	205.21
Temperature (K)	293(2)
Wavelength (Å)	0.71073
Crystal system space group	$P2_12_12_1$, orthorhombic
Unit cell dimensions (Å)	
a	9.213(3)
b	20.473(6)
c	5.202(1)
V (A^3)	981.2(5)
Z	4
D_{calc} (Mg/m^3)	1.389
Absorption coefficient (mm^{-1})	0.116
F (000)	440
Crystal size (mm)	0.3 × 0.2 × 0.2
Theta range (°)	2–25
Index ranges	$-10 \leqslant h \leqslant 10$, $-24 \leqslant k \leqslant 24$, $0 \leqslant l \leqslant 6$
Reflections collected/unique (R_{int})	2225/1509 (0.0257)
Completeness to 2 theta (%)	99.4
Refinement method	Full-matrix least-squares on F^2
Data restraint parameters	1509/11/166
Goodness-of-fit on F^2	1.091
Final *R* indices [$I > 2\sigma(I)$]	R_1 = 0.0605, wR_2 = 0.1483
R indices (all data)	R_1 = 0.0940, wR_2 = 0.1727

2.4. Ab initio quantum chemical calculations

The starting geometry for the quantum mechanical analyses has been considered from the crystal structures of the investigated systems.[6,10,11] The selection of basis set has been performed on similar compounds in our earlier work.[9] All crystal geometries were fully optimized using HF and B3LYP with 6-31+G* basis set level with Berny optimization algorithm. Systematic conformational search has been done around Φ_N (O-5–N1–C1′–C2′) in 12 steps of 30° each using the HF/6-31+G*//HF/6-31+G* and B3LYP/6-31+G*//6-31+G* levels of theory. During the calculations, all the geometries were completely allowed to relax including the amide nitrogen at planar geometry except the Φ_N torsion. The obtained energies were used to compute the relative energy with respect to the lowest minimum, and they were plotted as a function of Φ_N torsion to construct the potential energy curves. All the quantum chemical calculations were carried out using GAUSSIAN03.[17]

3. Results

3.1. Synthesis of XylβNHPr and ManβNHPr

Selective N-acylation of free β-D-glycopyranosylamines derived from xylose and mannose using propionic anhydride as the acylating agent afforded the title compounds, respectively, in good yields. The H-1 proton coupling constant value of 8.8 Hz for XylβNHPr and C-1 carbon chemical shift value of 77.8 ppm for ManβNHPr confirmed their β-anomeric configuration. Crystallization of these compounds from aqueous methanol furnished single crystals of XylβNHPr, whereas similar efforts were unsuccessful for Man analog.

3.2. Crystal structure of XylβNHPr and comparison with other xylosyl amides

3.2.1. Structure description

XylβNHPr (**1**) crystallized in the anhydrous state and its structure was solved in the space group $P2_12_12_1$. The ORTEP representation of the structure with atom numbering is shown in Figure 1. The pyranose ring adopts a $^4C_1$ conformation. Selected list of bond lengths, bond angles, and torsion angles is provided in Tables 2 and 3. These geometrical parameters are compared hereafter with those already reported for XylβNHAc (**3**)[6] and its tri-*O*-acetyl derivative, 3OAcXylβNHAc (**8**)[18] as shown in Figure 2. Among the sugar ring C–O distances observed for XylβNHPr, C1–O5 is longer than C5–O5 and a similar trend was noticed earlier for the propionamido derivatives, GlcNAcβNHPr and GlcβNHPr.[6] Most β-1-*N*-alkanamido sugar derivatives including XylβNHAc and 3OAcXylβNHAc exhibit a reverse trend in these bond lengths, due to the delocalization of the glycosidic N atom lone pair into the anti-bonding orbital of C1–O5. The extent of such delocalization may be lower in XylβNHPr. The N-glycosidic valence angle, O5–C1–N1, in XylβNHPr is smaller than that of C2–C1–N1 as seen earlier for all models and analogs of the N-glycoprotein linkage region.

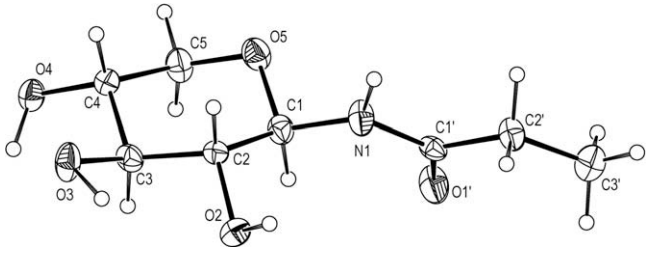

Figure 1. ORTEP representation (probability 30%) of crystalline structure of compound **1**.

3.2.2. Molecular conformation

A comparison of Φ_N values of several models and analogs is provided in Table 3. The observed values of torsions, Φ_N and Ψ_N, about C1–N1 and N1–C1′ bonds, respectively, are consistent with the *Z-anti* conformation of the amide group. The value (−101.2°) of the N-glycosidic torsion angle, Φ_N (O5–C1–N1–C1′), of XylβNHPr is found to be 20° smaller than that of the corresponding acetamide. Strangely enough for the tri-*O*-acetyl derivative of XylβNHAc, the value (−90.2°) of Φ_N turns out to be even less and matches well

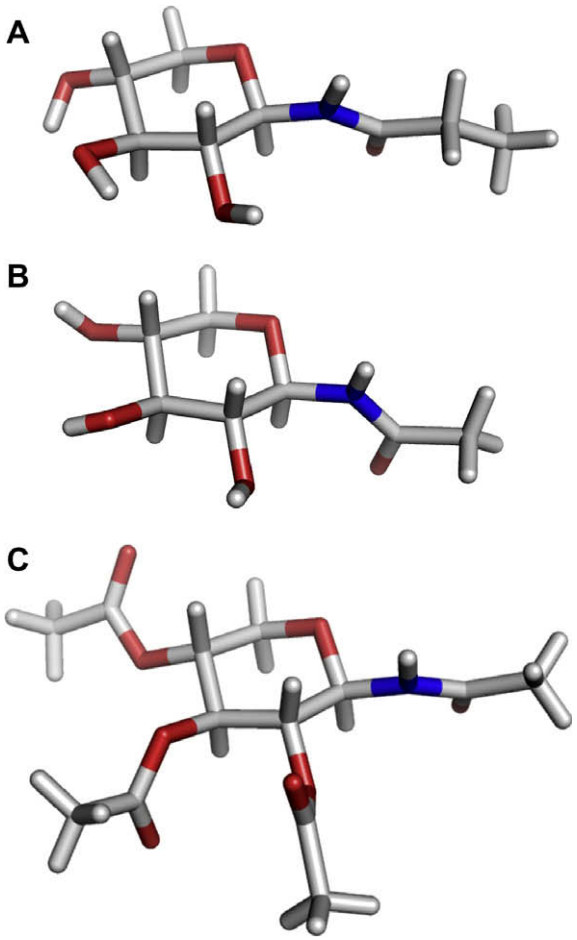

Figure 2. Comparison of crystal structures of different xyloside amines. A: XylβNHPr (**1**), B: XylβNHAc (**3**),[6] C: 3OAcXylβNHAc.[6]

Table 2
Selected bond lengths (Å) and bond angles (°) of compounds **1** and related xylosyl amide

Parameter	XylβNHPr (**1**)	XylβNHAc (**3**)[6]	3OAcXylβNHAc[18]
Bond lengths			
C1–O5	1.423(6)	1.418(3)	1.422(3)
C5–O5	1.413(6)	1.430(3)	1.431(5)
C1–N1	1.426(6)	1.435(3)	1.426(5)
C1′–N1	1.362(7)	1.336(3)	1.338(5)
C1′–O1′	1.241(6)	1.232(3)	1.223(5)
Bond angles			
O5–C1–N1	109.3(4)	107.85(15)	108.73(19)
C2–C1–N1	110.4(4)	111.74(17)	110.8(3)
N1–C1′–O1′	122.8(4)	121.6(2)	121.4(4)

Table 3
Selected torsion angles (°) of crystalline **1** and related compounds

Compound	Φ_N (O5–C1–N1–C1′)	Ψ_N (C1–N1–C1′–C2′)	χ_2 (N1–C1′–C2′–C3′)	Ref
GlcNAcβAsn·3H_2O	−98.9	180.0	−172.2	13
GlcNAcβNHAc·H_2O (**5**)	−89.8(5)	174.2(2)	—	10
GlcNAcβNHPr	−91.0(5)	172.5(5)	172.4(6)	11
GlcβAsn·H_2O	−83.6	174.0	−166.5	12
GlcβNHAc (**6**)	−93.8(2)	−179.2(3)	—	11
GlcβNHPr (**7**)	−89.5(5)	166.5(6)	114.7(8)	6
ManβNHAc (**4**)	−114.5(2)	171.3(2)	—	6
XylβNHAc (**3**)	−121.7(2)	−177.8(3)	—	6
XylβNHPr (**1**)	−101.2(6)	−176.6(5)	−176.6(5)	
3OAcXylβNHAc	−90.2(4)	177.4(3)	—	18

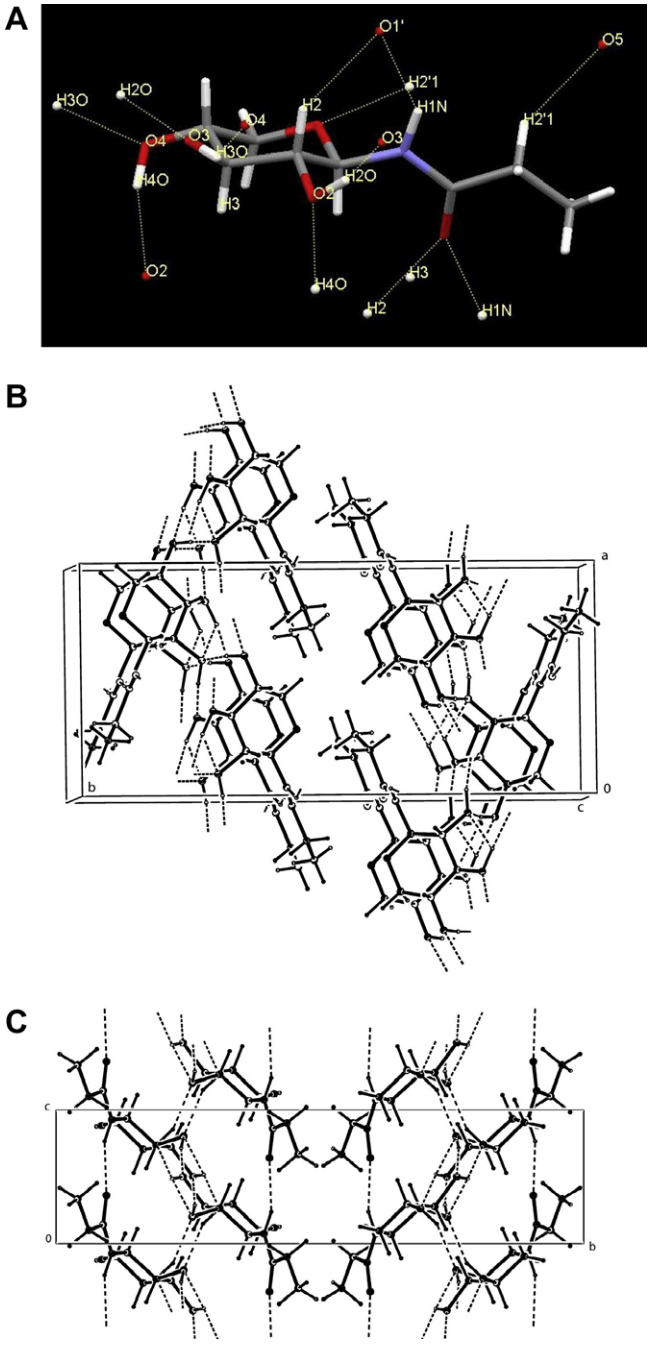

Figure 3. (A) Hydrogen bond network around compound **1** in the crystal structure. (B) and (C) Two different views of the crystal packing of compound **1** with hydrogen bonds represented as dashed lines.

with that of the model compound, GlcNAcβNHAc. The side chain torsion value, χ_2, of −176.6° observed for XylβNHPr points out the extended conformation of the aglycon moiety. The side chain of GlcNAcNHPr also takes up the same conformation, whereas that of the glucosyl analog, GlcNHPr, adopts a *gauche* conformation.[9]

3.2.3. Molecular packing

The various hydrogen bonds present in the crystal structure of XylβNHPr (**1**) were analyzed (Fig. 3) and their parameters listed in Table 4. The first and most notable feature is the occurrence of a finite chain of hydrogen bond connecting N1 directly with O1′ (Fig. 3C). Such a pattern is characteristic of GlcNAc derivatives.[8] The second feature is the infinite chain involving O2, O3, and O4 each of which acts as a donor as well as an acceptor (Table 5). Besides these regular hydrogen bonds, two C–H···O interactions are also seen to stabilize the molecular packing. The first of these involves C2′–H2′B of the propionamide side chain as the donor and ring oxygen O5 as the acceptor. The ability of O1′ to act as a bifurcated acceptor culminates in its interaction with C2–H in addition to being hydrogen bonded to N1–H. In sharp contrast, the molecular packing of XylβNHAc (**3**)[6] is essentially governed by a finite chain of regular hydrogen bonds starting from N1–H, running through O2, O4, and O3 and ending with O1′ and is devoid of any C–H···O interactions. In order to understand the reason(s) for the differences in Φ_N values between XylβNHPr (**1**) and XylβNHAc (**3**), a detailed study was performed using ab initio quantum chemical calculations.

3.3. Ab initio quantum chemical calculations

Ab initio calculations were performed using HF/6-31+G* since it was previously demonstrated that this basis set is well suited for compounds with neighboring *N*-acetyl groups.[9] The energy curves of six compounds as a function of Φ_N are described below (Fig. 4). The general tendency is the preference of the trans orientation when compared to the cis one. However, the range of allowed conformations is rather large, and clear differences can be observed depending on the monosaccharide or aglycon. Table 6 summarizes the different energy minima together with their associated energy values.

3.3.1. GlcNAcβNHAc (5)

The one-dimensional potential energy surface of acetamide derivative of GlcNAc (**5**) as a function of Φ_N variation shows that the minimum occurs at $\Phi_N \approx -150°$. An intramolecular hydrogen bond between the two *N*-acetyl groups stabilizes the energy minimum (Table 6). The region up to −90° from this global minimum is characterized by energetically quite flat surface with low energy range. It clearly shows that the GlcNAcβNHAc can easily make transitions among these conformational states by gaining some favorable interactions from the environment. A local minimum

has been found to occur at $\Phi_N \approx 90°$ with an energy of approx. 5 kcal/mol above the minimum. This conformer can easily move to the lowest energy region by crossing the barrier at 120° which occurs at a height less than 2 kcal/mol from the local minimum.

3.3.2. GlcβNHAc (6) and GlcβNHPr (7)

Absence of acetamido group at C2 position alters the low energy region of conformational energy space in compound **6**. In this case the lowest point of the energy curve has been found to occur at $\Phi_N \approx 180°$ with occurrence of O2–H···O1′ hydrogen bond. However, this conformer occurs at a height of 3.36 kcal/mol when acetamido group is present at C2 position. The next lowest minimum is found at $\Phi_N \approx -90°$ with a relative energy of about 0.11 kcal/mol. Rotational barrier between these two minima exists at a height of 0.91 kcal/mol at −120°. For this analog, the shape of the region from 90° to 180° is found to vary as compared to GlcNHAcβNHAc since it is almost flat. Minimization of the points corresponding to the global and the secondary minima was done to locate their exact position in the potential energy surface. It is observed from this result that the minima observed at $\Phi_N \approx -180°$ and $\Phi_N \approx -150°$ shifts to −165° and −92.2°, respectively. It is interesting to note here that the secondary minimum after complete minimization shows nearly equal value of Φ_N as observed in crystal structure (see Table 3). When comparing to GlcNAcβNHAc conformational behavior, it is noted that the absence of acetyl group at C2 position drastically reduces the torsional barrier at 120° due to free rotation without any hindrance by C2-acetamido carbonyl oxygen on C1-acetamido carbonyl oxygen, thereby making the torsional space a smoothened one.

The analysis of the Φ_N energy curve of the propionamide derivative **7** demonstrates a rather similar behavior as observed for the acetamide **6**. The presence of the extra methylene group in the latter system does not show any remarkable alteration on the potential energy surface except for the changes in the position of the observed lowest energy conformation. The lowest point of the curve occurs at $\Phi_N = -90°$ and the next lowest minimum occurs at $\Phi_N = 180°$ with a relative energy of 0.04 kcal/mol. A rotational barrier of about 1 kcal/mol is found at $\Phi_N \approx -120°$. This barrier is quite low for exchange of conformational state between the trans and *gauche* regions of the Φ_N torsional space.

3.3.3. ManβNHAc (4)

Scanning of Φ_N torsional space of the C2 epimer of GlcβNHAc reveals that the position of the lowest point $\Phi_N = -90°$ is conserved with respect to GlcβNHAc with alteration of the shape of the surface. Another minimum has been observed at $\Phi_N \approx 120°$ and is separated by higher energy barriers at 0° and 60°. This minimum occurs at a height of 0.7 kcal/mol from the lowest energy minimum position and is stabilized by an intra molecular O2–H···O1′ type hydrogen bond. Although the epimerization at C2 position does not alter the position of the lowest minimum significantly, it affects the barrier height and the shape of the surface significantly. Due to the axial position of O2, the intramolecular hydrogen bond O2–H···O1′occurs for Φ_N values close to 90° (instead of ca. 180° for the *gluco* configuration) and leads to the formation of an additional minimum, hence implying the importance of the C2 center of N-glycan models.

3.3.4. XylβNHAc (3) and XylβNHPr (1)

Φ_N conformational analysis of XylβNHAc reveals two minima at $\Phi_N \approx 180°$ and −90° with relative energies of 0 and 0.76 kcal/mol, respectively. The energy landscape presents a large plateau extending from +90° to −90°. The minimum at 180° is stabilized by an intramolecular hydrogen bond that occurs between O2–H and O1′.

Addition of a methylene group in the acetamido group (compound **1**) does not affect the preference for the trans arrangement. The conformational behavior of this compound is very similar to the one of XylβNHAc and the lowest energy conformation is also stabilized by the O2–H···O1′ hydrogen bond.

4. Discussion and conclusion

The ab initio calculations propose a constant low energy plateau between $\Phi_N = -90°$ and $\Phi_N = -180°$ for all compounds. The axial orientation of O2 of mannose results in a second minimum $\Phi_N = -180°$ stabilized by a hydrogen bond to the carbonyl oxygen of the aglycon group. For the other compounds with equatorial O2, this particular hydrogen bond occurs for $\Phi_N = 180°$ and explains the minimum observed in this region. The importance of this

Table 4
Regular and X–H···O hydrogen bonds in XylβNHPr (**1**)

Hydrogen bonds	H···A in Å	D···A in Å	∠DHA in °	Symmetry
N1–H···O1′	2.11	2.95	140	$x, y, z-1$
O2–H···O3	1.72	2.70	164	$x+½, -y+½, -z-1$
O3–H···O4	2.07	2.86	135	$x+½, -y+½, -z-1$
O4–H···O2	1.95	2.76	155	$x-½, -y+½, -z$
C2′–H2′B···O5	2.50	3.35	145	$-x+1, -y, z$
C2–H···O1′	2.33	3.18	143	$x, y, z-1$

Table 5
Regular hydrogen bonding patterns observed for the models and analogs

Compound name and No.	Finite chain H-Bonding	Infinite chain H-Bonding
GlcNAcβNHAc·1H$_2$O[10] (**5**)	N1–H1N···O1′ N2–H2N···O1″	···O1W–H1W···O3–H3O··· O6–H6O···...O1W–H2W··· O4–H4O···
GlcNAcβNHPr·1H$_2$O[6]	N1–H1N···O1′ N2–H2N···O1″	···O1W–H1W···O3–H3O··· O6–H6O···O1W–H2W··· O4–H4O...
GlcβNHAc[11] (**6**)	N1–H1N···O6–H6O···O2–H2O··· O3–H3O···O1′ O4–H4O···O5	No infinite chain
GlcβNHPr[6] (**7**)	N1–H1N···O6–H6O···O2–H2O··· O3–H3O···O1′ O4–H4O···O5	No infinite chain
XylβNHAc[6] (**3**)	N1–H1N···O2–H2O···O4–H4O··· O3–H3O···O1′	No infinite chain
XylβNHPr (**1**)	N1–H1N···O1′	···O2–H2O···O3–H3O···O4–H4O···
3OAcXylβNHAc[18] (**8**)	N1–H1N···O1′	No infinite chain

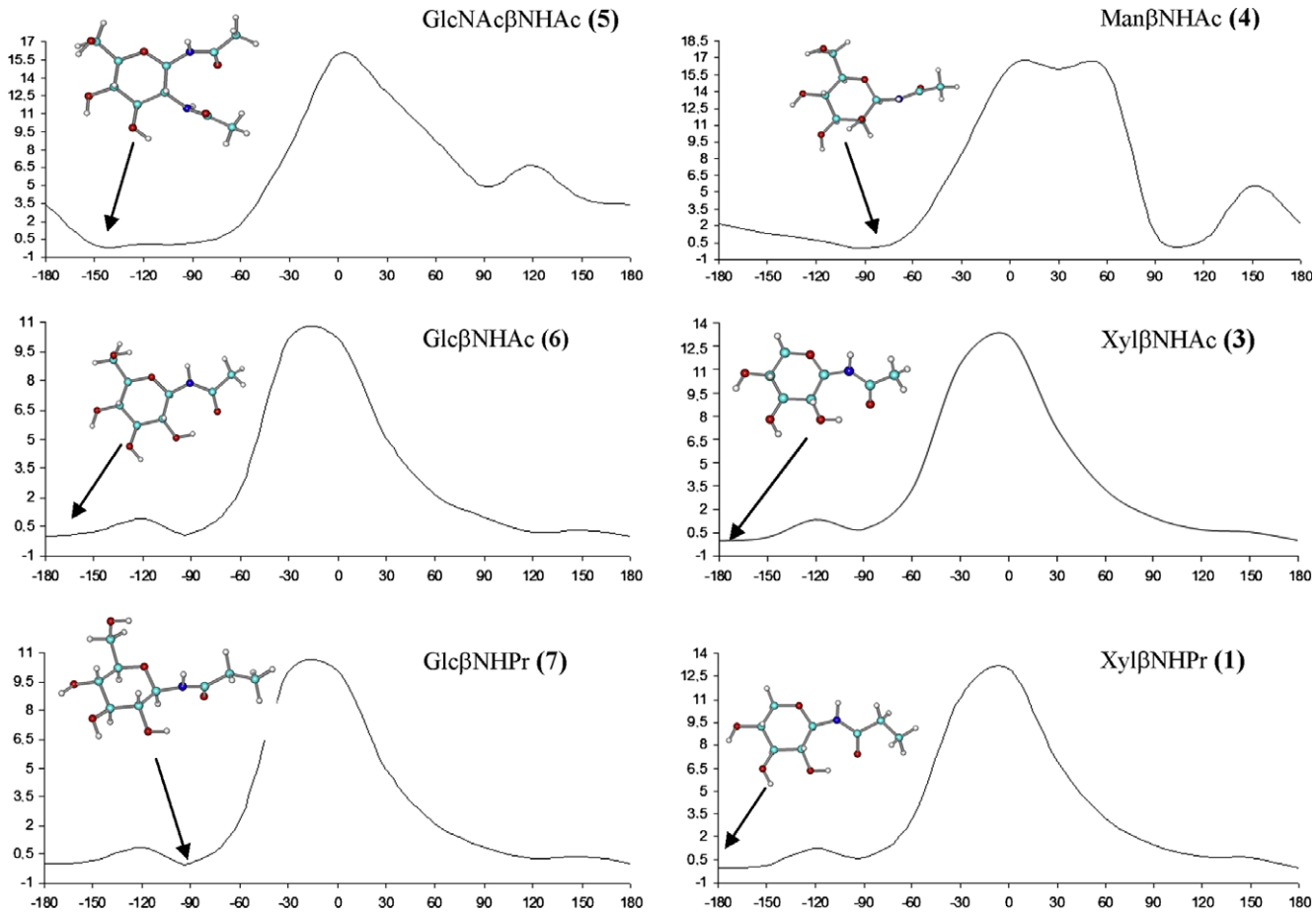

Figure 4. Quantum chemical energy variation of compounds **1**, **3**–**7** as a function of Φ_N.

Table 6
Selected HF/6-31+G* energy minima and computed hydrogen bonds

Compound	Φ_N (°)	E (rel) (kcal/mol)	H-Bond[b] (Å and (°))	Φ_N in crystal (°)	Ref.
GlcNAcβNHAc (**5**)	−150	0	2.55 (111.8)	−89.8	10
	−120	0.11			
	−90	0.15			
GlcβNHAc (**6**)	180(−165)[a]	0	1.85 (152)	−93.8	11
	−90(−92.2)[a]	0.11			
	120	0.21			
	150	0.28			
GlcβNHPr (**7**)	−90(−91.56)[a]	0		−89.5	6
	−180(−163.34)[a]	0.04	1.84 (152.1)		
	−150	0.12			
ManβNHAc (**4**)	−90	0		−114.5	6
	120	0.7	1.88 (139.8)		
XylβNHAc (**3**)	180	0	1.85 (152.3)	−121.7	
	−90	0.76			6
XylβNHPr (**1**)	180	0	1.84 (152.3)	−101.2	–
	−150	0.12			
	−90	0.59			
	−120	1.26			

[a] Torsion values after full optimization starting from the grid point.
[b] Intramolecular hydrogen bond between O2–H···O1′ (except for compound **5** with N2–H···O1′). Distance and angles (between parentheses) refer to H···O and X-H···O, respectively.

hydrogen bond on energy value is also demonstrated by the fact that the 'anti-clockwise' orientation of hydroxyl groups observed in all compounds of Figure 4 is the lowest energy one. Compound **5** with an *N*-acetyl group at position 2 has slightly different behavior with N2–H···O1′ hydrogen bond for Φ_N value of −150°. The importance of the nature of the substituent at C2 is therefore clearly demonstrated. On the contrary, there is no strong influence of the aglycone group (methyl or propyl) or of the group at C5 (*gluco* or *xylo*) on the conformational behavior of Φ_N. However, the situation is different in crystals, since these groups can influence the packing and therefore the environment of the *N*-acetamido group and its conformation.

The patterns of regular hydrogen bonding for three sets of acetamido- and propionamido derivatives of GlcNAc, Glc, and Xyl are listed in Table 5. The crystals of the acetamido- and propionamido derivatives of GlcNAc as well as Glc are isostructural in terms of the observed regular hydrogen bonding, whereas those of Xyl differ significantly. The direct hydrogen bonding between N1–H and O1′ appears to be a characteristic molecular recognition motif that controls Φ_N. Besides the variation in the regular hydrogen bonding patterns among the three xylopyranosyl derivatives, the weaker C–H···O interactions also lend a co-operative role in modulating the molecular conformation of the aglycon moiety in general and Φ_N in particular. While the acetamido derivative of Xyl exhibits no C–H···O interaction at all, the corresponding propionamido and the fully acetylated acetamido[18] derivatives show 2 and 3 C–H···O interactions, respectively, of varying types.

The predicted and experimental conformations of the Φ_N torsion angles of the different compounds have been reported in Table 6. The experimental values vary between −90° and −120°, therefore in a more narrow range than the theoretical ones. The intramolecular bond that stabilizes the trans conformation *in silico* does not occur in crystal state, where the other contacts are established with neighboring molecules as exemplified in compound **1** crystal structure where O2 gives hydrogen bound to O3 of a symmetry related molecule. It is also likely that in a water environment, the intramolecular contact will not be highly favored.

This comprehensive study illustrates for the first time the influence of neighboring groups and environmental factors particularly inter- and intramolecular interactions involving regular hydrogen bonds and the weak C–H···O contacts on the energy preference of the Φ_N torsion angle.

Acknowledgments

We are grateful to the Indo-French Centre for Promotion of Advanced Research (IFCPAR), New Delhi, for the financial support and encouragement. The authors (UA and DL) thank the Sophisticated Analytical Instrumentation Facility (SAIF), IIT, Madras, for the X-ray data collection and Dr. Babu Varghese for his valuable technical help.

Supplementary data

Complete structural data of the XylβNHPr have been deposited at the Cambridge Crystallographic Data Centre (CCDC # 703153), and can be obtained free of charge via www.ccdc.cam.ac.uk/data_request/cif (or from the Cambridge Crystallographic Data Centre, 12 Union Road, Cambridge CB21EZ, UK; fax: (+44) 1123-336-033; or email: deposit@ccdc.cam.ac.uk). Supplementary data associated with this article can be found, in the online version, at doi:10.1016/j.carres.2008.11.013.

References

1. Dwek, R. A. *Chem. Rev.* **1996**, *96*, 683–720.
2. Varki, A. *Glycobiology* **1993**, *3*, 97–130.
3. Spiro, R. G. *Glycobiology* **2002**, *12*, 43R–56R.
4. Imberty, A.; Pérez, S. *Protein Eng.* **1995**, *8*, 699–709.
5. Petrescu, A. J.; Milac, A. L.; Petrescu, S. M.; Dwek, R. A.; Wormald, M. R. *Glycobiology* **2004**, *14*, 103–114.
6. Lakshmanan, T.; Sriram, D.; Priya, K.; Loganathan, D. *Biochem. Biophys. Res. Commun.* **2003**, *312*, 405–413.
7. Loganathan, D.; Aich, U. *Glycobiology* **2006**, *16*, 343–348.
8. Loganathan, D.; Aich, U.; Lakshmanan, T. *Proc. Indian Nat. Sci. Acad.* **2005**, *71A*, 213–236.
9. Mohamed Naseer Ali, M.; Aich, U.; Varghese, B.; Pérez, S.; Imberty, A.; Loganathan, D. *J. Am. Chem. Soc.* **2008**, *130*, 8317–8325.
10. Sriram, D.; Lakshmanan, T.; Loganathan, D.; Srinivasan, S. *Carbohydr. Res.* **1998**, *309*, 227–236.
11. Sriram, D.; Srinivasan, H.; Srinivasan, S.; Priya, K.; Vishnu Thirtha, M.; Loganathan, D. *Acta Crystallogr., Sect. C* **1997**, *53*, 1075–1077.
12. Delbaere, L. T. *Biochem. J.* **1974**, *143*, 197–205.
13. Ohanessian, J.; Avenel, D.; Neuman, A.; Gillier-Pandraud, H. *Carbohydr. Res.* **1980**, *80*, 1–13.
14. Isbell, H. S.; Frush, H. L. *J. Org. Chem.* **1958**, *23*, 1309–1315.
15. Sheldrick, G. M., University of Gottingen, 1997.
16. Spek, A. L. *J. Appl. Crystallogr.* **1988**, *21*, 578.
17. Frisch, M. J. X., Gaussian: Wallingford, CT, 2004.
18. Avalos, M.; Babiano, R.; Carretero, M. J.; Cintas, P.; Higes, F. J.; Jimenez, J. L.; Palacios, J. C. *Tetrahedron* **1998**, *54*, 615–628.